Crystalline Chromium Electroplating with High Current Efficiency Using Chloride Hydrate Melt-Based Trivalent Chromium Baths

Ken ADACHI[a], Atsushi KITADA*[a], Kazuhiro FUKAMI[a]1, Kuniaki MURASE[a]1

[a] Department of Materials Science and Engineering

Kyoto University

Sakyo-ku, Kyoto 606-8501, Japan

* corresponding author; kitada.atsushi.3r@kyoto-u.ac.jp

1 ISE member

Keywords: Trivalent chromium electrodeposition; Hydrate melt; Crystalline chromium; Current efficiency

Abstract

Chromium (Cr) plating using trivalent chromium has been investigated as a replacement for the highly-toxic hexavalent chromium bath. Herein, we report novel chromium plating baths using hydrate-melts. Hydrate-melts have been investigated in recent years as an electrolyte for aqueous Li-ion batteries with a wide electrochemical window, and can be used as an electroplating bath in which the reduction of protons, i.e., bath decomposition, is suppressed. By using a hydrate-melt for electroplating with trivalent chromium, the increase of local pH during electrolysis is suppressed and generation of the electrochemically-inert oligomer of chromium hydroxide can be avoided. Crystalline chromium electrodeposits were successfully obtained from the hydrate-melt-based aqueous baths, which had not been possible with the conventional trivalent chromium process requiring organic coordination agents. Moreover, a current efficiency greater than 80% was achieved. The hydrate-melt-based aqueous bath, with low material cost, is a promising candidate for industrial trivalent chromium plating.

1. Introduction

Chromium plating, especially at thicknesses greater than 2 μm, is industrially important. Its excellent corrosion and wear resistance offer a long-lasting and durable surface [1,2]. The current industrial process for thick chromium plating is based on aqueous solutions of highly-toxic hexavalent chromium acid [3]. The risks to human health and to the environment have led to legislation against Cr(VI), e.g., RoHS and REACH restrictions in the EU and similar regulations in the USA, China, Japan and elsewhere. Trivalent chromium plating, which uses the less-toxic Cr(III), has been investigated as a candidate for an alternative, environmentally benign process.

Electroplating of chromium in an aqueous bath is inevitably accompanied by hydrogen evolution due to the negative electrode potential (Cr^{3+} + 3e = Cr, $E°$ = –0.744 V *vs*. SHE) [4]. This hydrogen evolution decreases the current efficiency of the electroplating process. It also increases local pH near the cathode, resulting in production by olation of an electrochemically-inert oligomer of hydroxo-bridged complexes of chromium, lowering the plating rate [5–10]. For these reasons, trivalent chromium plating requires additives to avoid the local pH increase and/or olation.

Many studies on aqueous trivalent chromium baths have focused on the use of organic complexing agents such as formic acid and oxalic acid, which form stable chromium complexes at high pH [11–21]. Additionally, non-aqueous trivalent chromium baths have been studied using organic solvents, deep eutectic solvents and ionic liquids [22–29], which can decrease hydrogen evolution. The lower material cost and the air/moisture sensitivity have been of particular interest for practical use [28,29]. However, the chromium electrodeposits from existing trivalent chromium baths are non-crystalline and mixture of chromium and chromium carbide [30-32], due to contamination by organic compounds, which results in reduced physical properties compared with the crystalline chromium usually obtained from hexavalent chromium baths [1,33]. Consequently, novel trivalent chromium baths that do not require use of organic reagents are of great interest.

We examined hydrate-melt based baths composed of inorganic salts as a novel approach for trivalent chromium plating. Studies of the solution chemistry of hydrate-melts date back to the reports by Angel *et al.* in the 1960s [34]. In recent years, many studies have been carried out on the use of hydrate-melts as “Water-in-Salt” electrolytes for aqueous Li-ion batteries, with a wide electrochemical window [35-37]. Most of the H_2O molecules in hydrate-melts coordinate to the ions of the component of the salt,[38] which increases their electrochemical stability. However, only a few reports [39-41] on the

use of hydrate-melt as an electroplating bath have been published. By using hydrate-melt as the plating bath for trivalent chromium plating, the hydrogen evolution and the olation of Cr(III) should be suppressed. In this study, the electrochemistry of trivalent chromium in hydrate-melts of Li-Cr(III) and Ca-Cr(III) chlorides and the associated electrodeposition behavior were investigated. Despite its higher cost compared with other chloride compounds such as $CaCl_2$ or $MgCl_2$, we mainly investigated the hydrate-melt of LiCl since lithium hydroxide scarcely precipitates by hydrolysis due to the increase of local pH during electrolysis.

2. Experimental method

The series of H_2O-LiCl-$CrCl_3$ electrolytes and H_2O-LiCl electrolytes with different H_2O/LiCl molar ratios (= *n*) and their pH values, the conductivities and the viscosities at 50°C are shown in Table I and Table II. The electrolytes were prepared by adding LiCl (98.0% purity, FUJIFILM Wako Pure Chemical Corporation) and $CrCl_3 \cdot 6H_2O$ (93.0% purity, FUJIFILM Wako) to deionized water. All reagents were used as purchased. These solutions containing $CrCl_3$ show low pH value because the water molecules strongly coordinated to the Cr^{3+} ions, which tend to be dissociated to provide H^+. By adding small amounts of hydrochloric acid (35-37% purity, Nacalai Tesque), the pH values of H_2O-LiCl electrolytes were made similar to those of the H_2O-LiCl-$CrCl_3$ electrolytes. For chromium electroplating tests, H_2O-LiCl-$CrCl_3$ electrolytes containing boric acid (H_3BO_3) were prepared by adding the reagent (99.5% purity, FUJIFILM Wako). H_3BO_3 is a typical pH buffering agent used to prevent the precipitation of metal hydroxides during electroplating. Although the pK_a (acid dissociation constant) of H_3BO_3 is 8-9, it is empirically known that it can prevent precipitation of metal hydroxides even in acidic region like the case of Watts nickel plating bath [42].

Electrolysis was carried out with the electrolyte at 50 °C in air. Prior to electrolysis, the electrolyte was degassed by N_2 bubbling for 20 min. In the same procedure, H_2O-$CaCl_2$-$CrCl_3$ electrolytes with different H_2O/$CaCl_2$ molar ratios (= *n*) were prepared using $CaCl_2$ (95% purity, FUJIFILM Wako) (see Table SI). The pH values, the conductivities and the viscosities of the electrolytes were measured using pH meter (HORIBA Laquaact D-71), conductivity meter (HORIBA 3553-10D) and viscometer (Kyoto Electronics Manufacturing, EMS-1000).

Electrochemical measurements were performed using a potentiostat (Bio-Logic Science Instruments, SP-50) with a typical three-electrode cell; Ni plated substrate (15×20 mm^2) as the working electrode

(WE), glassy carbon block as the counter electrode (CE), and Ag|AgCl (HORIBA, 2565A) in 3.33 mol dm^{-3} KCl aqueous solution with a salt bridge as the reference electrode (RE). The Ni plated substrates were prepared using brass sheet (0.5 mm thickness and 15×25 mm^2) pre-treated with degreasing solution (Okuno Chemical Industries, Ace Clean 850), and electrolysis was carried out in a Watts bath [42] at a current density of 50 mA cm^{-2} for 10 min to fabricate a matte Ni film with a thickness of about 10 μm. To compensate for the ohmic drop between WE and RE, the solution resistance was determined by electrochemical impedance spectroscopy (EIS) measurements at a frequency of 100 kHz and AC voltage amplitude of 20 mV, noting that the electrochemical cell was arranged to make the positions of WE and RE near to reduce ohmic drop, resulting in the certain differences of the ohmic drops for each measurement.

The deposits obtained thorough electrolysis were characterized by X-ray diffraction (XRD) with Cu *K*α (1.542 Å) using a RIGAKU RINT2200, scanning electron microscope (SEM) observation using a KEYENCE VE-7800, energy dispersive X-ray spectrometry (EDX) using an EDAX Element, and transmission electron microscopy (TEM) analysis using a JEOL JEM-2010. The samples for TEM analysis were prepared by focused ion beam (FIB) using a SII Nanotechnology Inc. SMI9200.

3. Results and discussion

3.1 Electrochemical measurements

Linear sweep voltammograms (LSV) for each H_2O-LiCl-$CrCl_3$ electrolyte measured are shown in Fig. 1a, and those with ohmic compensation in Fig. 1b. In the case of “LiCl-free,” the onset of cathodic current appeared at around –0.4 V *vs*. Ag|AgCl and monotonically increased with the cathodic overvoltage. The gas generation at the electrode suggested that this cathodic current was mainly due to the H^+ reduction and hydrogen evolution. For n = 3, 5, and 10, however, the cathodic currents initially increased, and then remained constant until the potential reached around –1.0 V. As the LiCl concentrations increased, the constant values of the current densities decreased. Below –1.1 V, the cathodic current increased sharply. These results show that H_2 generation, i.e., bath decomposition, was suppressed in the presence of a copious amount of LiCl.

Korshunov *et al*. used the mercury static electrode with a large overvoltage for H^+ reduction to study the electrochemical behavior of trivalent chromium in concentrated LiCl aqueous solution [7]. The peaks of cathodic current derived from the reduction of trivalent chromium to divalent chromium

appeared at around –0.5 V *vs.* Ag|AgCl. In Fig. 1, however, such peaks could not be detected due to the comparably large background currents of the H^+ reduction as the Ni-plated substrate was used.

To confirm the effect of LiCl concentration on the bath decomposition, blank tests were performed using the baths without $CrCl_3$. A set of LSV using the H_2O-LiCl-HCl electrolytes of different LiCl-concentrations measured is shown in Fig. 2a, and that with ohmic compensation is shown in Fig. 2b. The H^+ reduction behavior depended on n. At lower LiCl concentrations (n = 100 and 10) the cathodic current monotonically increased below –0.5 V, while at higher LiCl concentrations (n = 5 and 3) substantial cathodic currents were observed below –1.1 V. This result clearly shows that the H^+ reduction was suppressed by the presence of concentrated LiCl. The suppression of H^+ reduction was not due to thermodynamic factors because the differences in pH of these H_2O-LiCl-HCl electrolytes of n = 3, 5 and n = 10, 100 were not more than 1, which cannot explain the difference in onset potentials of cathodic current of more than 0.5 V. For these reasons, the suppression of H^+ reduction in H_2O-LiCl-$CrCl_3$ electrolytes of n = 3, 5 was mainly due to kinetic factors: the lack of free H_2O molecules caused slow H^+ diffusion and tight H^+ supply to the electrode, resulting in the low limiting current. As shown in Fig. S1a, the LSVs were measured in H_2O-$CaCl_2$-$CrCl_3$ and pH-adjusted H_2O-$CaCl_2$ electrolytes with a H_2O / $CaCl_2$ molar ratio of 10, using the same setup. Similar tendencies were observed; the cathodic current of the H^+ reduction was suppressed due to the presence of a copious amount of $CaCl_2$ compared with the LSV measured in the $CaCl_2$-free electrolyte of H_2O-$CrCl_3$ until the potential reached around –1 V, and the cathodic current increased below –1.1 V in H_2O-$CaCl_2$-$CrCl_3$ electrolyte, suggesting that the suppression of H^+ reduction is common in hydrate-melt chloride compounds.

Fig. 3 shows a series of cyclic voltammograms (CVs) with different cathodic switching potentials. The CVs for H_2O-LiCl-$CrCl_3$ electrolytes of n = 3, 5, 10 with the switching potentials of –0.7 V, –1.0 V and –1.3 V without ohmic compensation are shown in Fig. 3a (i-iii), and those with ohmic compensation are shown in Fig. 3b (i-iii). For the CVs with switching potentials of –0.7 V and –1.0 V, anodic currents were scarcely observed for the anodic scans. However, for the CVs with the switching potentials of –1.3 V, anodic currents were observed from –0.8 V to –0.6 V. From these results, the cathodic currents below –1.0 V during the cathodic scans and the anodic currents above –0.8 V during the anodic scans were, respectively, due to the electrodeposition and the anodic dissolution of metallic chromium, which strongly suggests successful electrodeposition of metallic chromium in all H_2O-

$LiCl\text{-}CrCl_3$ electrolytes. This is because the H^+ reduction and the increase of local pH near the cathode were suppressed by the kinetic factors mentioned above, preventing the olation of hydroxo-bridged complexes of chromium.

3.2 Characterization of the deposits

Galvanostatic electrolysis using $H_2O\text{-}LiCl\text{-}CrCl_3$ electrolytes of n = 3, 5, and 10 was conducted to obtain electrodeposits. Photographs and SEM images of the deposits are shown in Fig. 4a (i-iii). Black and/or gray colored deposits covered with fine particles of grain size less than 1 μm were obtained. The XRD patterns are shown in Fig. 4b. The deposits obtained using electrolytes of n = 3 and 5 were measured with the Ni plated substrate, and that obtained using electrolyte n = 10 was separated from the Ni plated substrate and measured with a glass substrate. The deposits corresponded to metallic chromium. Although *hexavalent* chromium plating is generally composed of an α-Cr phase of bcc structure, these deposits contained δ-Cr phase of A15-type cubic structure. According to the literature, metallic chromium of δ-Cr phase has been obtained through vaporization of metals in an Ar atmosphere or in vacuum [43,44], and through heat treatment of amorphous electrodeposits originally prepared from an organic solvent bath [45]. Since these preparation conditions are different from the current work, the mechanism of the formation of metastable δ-Cr phase remains unclear. The EDX spectra of the deposits shown in Fig. 4c indicate that they were mainly composed of chromium and of certain amounts of Cl and O as mentioned below. The presence of Cl and O suggests an increase in chromium hydroxide or chromium chloride generated by the hydrolysis reaction due to the increase of local pH in the vicinity of the cathode [8].

To avoid increases in impurities and to avoid an increase of local pH, H_3BO_3 was added as a typical pH buffer. H_3BO_3 of 30 g dm^{-3} was added to $H_2O\text{-}LiCl\text{-}CrCl_3$ electrolytes of n = 3, 5 and 10, which were then used for galvanostatic electrodeposition. Photographs and SEM images of the deposits are shown in Fig. 5a (i-iii). Smooth and gray films with a metallic luster were obtained for electrolytes n = 3 and 5, composed of particles with a grain size of several microns, as seen in the SEM image in Fig. 5a (i-ii). However, for the electrolyte n = 10, as shown in Fig. 5a (iii), blackish deposits composed of particles with a grain size of several microns or submicrons were obtained. The EDX spectra shown in Fig. 5c indicate that the intensities of Cl and O were much smaller than those of the deposits prepared without H_3BO_3. Therefore, the precipitation and increases in chromium hydroxide and

chromium chloride were significantly suppressed by adding H_3BO_3. Among n = 3, 5 and 10, the intensity of O was highest for n = 10. This was because the concentration of LiCl was not sufficient to form a hydrate-melt in which H^+ reduction could be suppressed, despite the presence of H_3BO_3, leading to the precipitation and increases in impurities and the black appearance of the deposits. The XRD patterns of the deposits prepared from the electrolytes with H_3BO_3 are shown in Fig. 5b. The deposits were composed of mainly α-Cr phase and partially δ-Cr phase, as in the case without H_3BO_3.

To clarify the effect of H_3BO_3, high-angle annular dark field-scanning TEM (HADDF-STEM) images of sample cross-sections were collected. Fig. 6a shows the images for H_2O-LiCl-$CrCl_3$ electrolytes of (i) n = 3 and (ii) n = 5 without H_3BO_3 and Fig. 6b shows those for H_2O-LiCl-$CrCl_3$ electrolytes with H_3BO_3 (i) n = 3 and (ii) n = 5. Each inset shows typical electron diffraction (SAED) patterns of the deposits. As shown in Fig. 6a (i, ii), the deposits prepared from H_2O-LiCl-$CrCl_3$ electrolytes without H_3BO_3 were composed of two kinds of domain, with white and black appearances. The SAED patterns of white domains corresponded to the pattern of highly crystalline chromium with a bcc-structure, and those of the black domains showed only halos indicating them to be amorphous. While the deposits prepared from the electrolytes with H_3BO_3 were composed of homogeneous crystalline chromium, those prepared from the electrolytes without H_3BO_3 contained some amorphous domains. These compositions were examined by TEM-EDX analysis, as shown in Fig. 7. The TEM-EDX analyses showed molar ratios of Cr:O:Cl = 97:3:0 for the white domains (Fig. 7a) and Cr:O:Cl = 31:64:5 for the black domains (Fig. 7b). This indicated that the white domains were crystalline chromium with slight Cl impurities and the black domains were mixtures of chromium compounds such as oxides, hydroxides, and chlorides.

Similar results were obtained using $CaCl_2$ analogous electrolytes, as shown in Fig. S1b-d.

3.3 Current efficiency and plating rate

Fig. 8 shows photographs and SEM images of cross-sections of the chromium deposits prepared at several current densities using the H_3BO_3-added electrolytes with (a i-iv) n = 3 and (b i-iv) n = 5. All deposits had a gray-colored smooth surface and uniform thickness. The adhesion of the edge of the deposits was decreased, especially for n = 3. Fig. 9 displays the current efficiency and the plating rate. The current efficiencies were calculated using the weight of the deposits and by assuming the half-cell reaction of the electrodeposition of chromium to be Cr(III) + 3e = Cr. The plating rates were calculated

using the thickness of the deposits obtained from the SEM images.

As shown in Fig. 9a, the current efficiencies of chromium electrodeposition were approximately 60–80% for n = 3 and 20–60% for n = 5, which was consistent with the cathodic current due to the H^+ reduction being more suppressed in n = 3 than in n = 5 as the LSV showed in Fig. 1. It is worth noting that the current efficiency increased with current density because the H^+ reduction took place in a diffusion-limited condition, resulting in a maximum current efficiency of 83% for n = 3. As shown in Fig. 9b, the plating rate for n = 5 was higher than that for n = 3, with a maximum value of 0.3 μm min^{-1}. Although no proper benchmark for industrial trivalent chromium plating has been established yet, the reported current efficiencies in some studies are less than 50% [11,12], and the plating rate of industrial *hexavalent* chromium plating is 0.1–0.3 μm min^{-1} [1], which emphasizes the advantages of the LiCl hydrate melt-based electrolyte.

The most valuable property of the H_2O-LiCl-$CrCl_3$ bath is the suppression of H^+ reduction during electrolysis. This allows for electrodeposition of crystalline chromium with low levels of impurities that have not been achievable with the conventional trivalent chromium processes using organic ligands or non-aqueous electrolytes. The high current efficiency and plating rate are also attractive. Further research and application of this hydrate-melt bath to the electrodeposition of metals other than chromium is anticipated.

4. Conclusions

We investigated the hydrate-melt-based trivalent chromium aqueous bath. Very high concentrations of LiCl or $CaCl_2$ suppressed H^+ reduction. By adding H_3BO_3 as a typical pH buffer, the increase of local pH was suppressed sufficiently, which allowed for electrodeposition of chromium without generating an electrochemically-inert chromium oligomer. From the organics-free H_2O-LiCl-$CrCl_3$ electrolytes, crystalline chromium with high purity was successfully electrodeposited at a high current efficiency of more than 80%. The use of metal chloride hydrate-melts for electroplating bath is a novel scheme for suppressing hydrogen evolution and local pH increase, without using organic complexing agents.

Acknowledgments

This work was supported financially by Grants-in-Aid for Scientific Research (B) (No.19H02490: A. K.) from the Japan Society for the Promotion of Science (JSPS). K.M is grateful for financial support from the Kyoto University Foundation.

References

[1] M. Schlesinger, M. Paunović, Modern Electroplating (5th edition), John Wiley & Sons, 2011, p. 205.

[2] N. Kanani, Electroplating: basic principles, processes and practice (2nd edition), Elsevier Advanced Technology, Amsterdam, 2004, p. 133.

[3] D. L. Perry, Handbook of inorganic compounds (2nd edition), CRC Press, Boca Raton, 2011.

[4] D. R. Lide, CRC handbook of physics and chemistry (84th edition), CRC Press, Boca Raton, 2003.

[5] S. Survilienė, O. Nivinskienė, A. Češunienė, A. Selskis, Effect of Cr(III) solution chemistry on electrodeposition of chromium, J. Appl. Electrochem. 36 (2006) 649.

[6] A.A. Edigaryan, V. A. Safonov, E. N. Lubnin, L. N. Vykhodtseva, G. E. Chusova, Y. M. Polukarov, Properties and preparation of amorphous chromium carbide electroplates, Electrochim. Acta 47 (2002) 2775.

[7] V. N. Korshunov, L. N. Vykhodtseva, V. A. Safonov, Reduction of trivalent chromium ions on stationary mercury electrode in concentrated LiCl solutions, Russ. J. Electrochem. 40 (2004) 466.

[8] S. Surviliene, V. Jasulaitiene, O. Nivinskiene, A. Češuniene, Effect of hydrazine and hydroxylaminophosphate on chrome plating from trivalent electrolytes, Appl. Surf. Sci. 253 (2007) 6738.

[9] N. V. Mandich, Chemistry of chromium, in: AESF 82nd Tech. Conf. SURFIN95, Baltimore, Md, 1995, Vol. 82, American electroplaters and surface finishers society, 1995, p. 909.

[10] M. R. Grace, L. Spiccia, Kinetics of anation of Cr(III) hydrolytic oligomers: reaction of dimer with sulfate, Inorg. Chim. Acta 213 (1993) 103.

[11] V. S. Protsenko, F. I. Danilov, V. O. Gordiienko, S. C. Kwon, M. Kim, J. Y. Lee, Electrodeposition of hard nanocrystalline chrome from aqueous sulfate trivalent chromium bath, Thin Solid Films 520 (2011) 380.

[12] Y. B. Song, D. T. Chin, Current efficiency and polarization behavior of trivalent chromium electrodeposition process, Electrochim. Acta 48 (2002) 349.

[13] M. R. Bayati, M. H. Shariat, K. Janghorban, Design of chemical composition and optimum working conditions for trivalent black chromium electroplating bath used for solar thermal collectors, Renew. Energy 30 (2005) 2163.

[14] Z. Tu, Z. Yang, J. Zhang, M.Z. An, W. L. Li, Cathode Polarization in Trivalent Chromium Plating,

Plat. Surf. Finish. 80 (1993) 79.

[15] N. V. Phuong, S. C. Kwon, J. Y. Lee, J. Shin, B.T. Huy, Y. I. Lee, Mechanistic study on the effect of PEG molecules in a trivalent chromium electrodeposition process, Microchem. J. 99 (2011) 7.

[16] Z. Zeng, L. Wang, A. Liang, J. Zhang, Tribological and electrochemical behavior of thick Cr–C alloy coatings electrodeposited in trivalent chromium bath as an alternative to conventional Cr coatings, Electrochim. Acta 52 (2006) 1366.

[17] F. I. Danilov, V. S. Protsenko, T. E. Butyrina, E. A. Vasil'eva, A. S. Baskevich, Electroplating of chromium coatings from Cr(III)-based electrolytes containing water soluble polymer, Prot. Met. 42 (2006) 560.

[18] Z. Zeng, Y. Sun, J. Zhang, The electrochemical reduction mechanism of trivalent chromium in the presence of formic acid, Electrochem. Commun. 11 (2009) 331.

[19] J. McDougall, M. El-Sharif, S. Ma, Chromium electrodeposition using a chromium(III) glycine complex, J. Appl. Electrochem. 28 (1998) 929.

[20] I. Drela, J. Szynkarczuk, J. Kubicki, Electrodeposition of chromium from Cr (III) electrolytes in the presence of formic acid, J. Appl. Electrochem. 19 (1989) 933.

[21] J. Szynkarczuk, I. Drela, J. Kubicki, Electrochemical behaviour of chromium(III) in the presence of formic acid—I, Electrochim. Acta 34 (1989) 399.

[22] A. P. Abbott, A. A. Al-Barzinjy, P. D. Abbott, G. Frisch, R. C. Harris, J. Hartley, K. S. Ryder, Speciation, physical and electrolytic properties of eutectic mixtures based on $CrCl_3 \cdot 6H_2O$ and urea, Phys. Chem. Chem. Phys. 16 (2014) 9047.

[23] W.H. Wade, L.F. Yntema, The Electrodeposition of Chromium from Trivalent Salt Solutions, Trans. Electrochem. Soc. 74 (1938) 461.

[24] A. P. Abbott, G. Capper, D. L. Davies, R. Rasheed, Ionic Liquids Based upon Metal Halide/Substituted Quaternary Ammonium Salt Mixtures, Inorg. Chem. 43 (2004) 3447.

[25] S. Eugénio, C. M. Rangel, R. Vilar, S. Quaresma, Electrochemical aspects of black chromium electrodeposition from 1-butyl-3-methylimidazolium tetrafluoroborate ionic liquid, Electrochim. Acta 56 (2011) 10347.

[26] S. Survilienė, S. Eugénio, R. Vilar, Chromium electrodeposition from [BMIm][BF_4] ionic liquid, J. Appl. Electrochem. 41 (2011) 107.

[27] C. Du, B. Zhao, X. B. Chen, N. Birbilis, H. Yang, Effect of water presence on choline chloride-

2urea ionic liquid and coating platings from the hydrated ionic liquid, Sci. Rep. 6 (2016) 29225.

[28] L.S. Bobrova, F. I. Danilov, V. S. Protsenko, Effects of temperature and water content on physicochemical properties of ionic liquids containing $CrCl_3 \cdot xH_2O$ and choline chloride, J. Mol. Liq. 223 (2016) 48.

[29] E. S. C. Ferreira, C. M. Pereira, A. F. Silva, Electrochemical studies of metallic chromium electrodeposition from a Cr(III) bath, J. Electroanal. Chem. 707 (2013) 52.

[30] L. N. Vykhodtseva, A. A. Edigaryan, E. N. Lubnin, Y. M. Polukarov, "Composition, Structure, and Corrosion–Electrochemical Properties of Chromium Coatings Deposited from Chromium(III) Electrolytes Containing Formic Acid and Its Derivatives", Russ. J. Electrochem. 40, (2004) 387.

[31] E. N. Lubnin, A. A. Edigaryan, Y. M. Polukarov, "X-ray photoelectron spectroscopy of chromium layers electroplated from oxalate-sulfate solutions", Prot. Met. 36, (2000) 301.

[32] V. A. Safonov, L. N. Vykhodtseva, Y. M. Polukarov, O. V. Safonova, G. Smolentsev, M. Sikora, S. G. Eeckhout and P. Glatzel, "Valence-to-Core X-ray Emission Spectroscopy Identification of Carbide Compounds in Nanocrystalline Cr Coatings Deposited from Cr(III) Electrolytes Containing Organic Substances", J. Phys. Chem. B. 110, (2006) 23192.

[33] K. Watanabe, Decorative Trivalent Chromium Plating, J. Surf. Finish. Soc. Japan 56 (2005) 320. (doi:10.4139/sfj.56.320)

[34] C. A. Angell, A new class of molten salt mixtures the hydrated dipositive ion as an independent cation Species, J. Electrochem. Soc. 112 (1965) 1224.

[35] L. Suo, Y. S. Hu, H. Li, M. Armand, L. Chen, A new class of Solvent-in-Salt electrolyte for high-energy rechargeable metallic lithium batteries, Nat. Commun. 4 (2013) 1481.

[36] L. Suo, O. Borodin, T. Gao, M. Olguin, J. Ho, X. Fan, C. Luo, C. Wang, K. Xu, "Water-in-salt" electrolyte enables high-voltage aqueous lithium-ion chemistries, Science 350 (2015) 938.

[37] Y. Yamada, K. Usui, K. Sodeyama, S. Ko, Y. Tateyama, A. Yamada, Hydrate-melt electrolytes for high-energy-density aqueous batteries, Nat. Energy 1 (2016) 16129.

[38] L. Greenspan, Humidity Fixed Points of Binary Saturated Aqueous Solutions, J. Res. Natl. Bur. Stand. Phys. Chem. 81 (1977) 89.

[39] A. Uehara, O. Shirai, T. Fujii, T. Nagai, H. Yamana, Electrochemical deposition of uranium oxide in highly concentrated calcium chloride, J. Appl. Electrochem. 42 (2012) 455.

[40] Q. Huang, T. W. Lyons, Electrodeposition of rhenium with suppressed hydrogen evolution from

water-in-salt electrolyte, Electrochem. Commun. 93 (2018) 53.

[41] K. Adachi, A. Kitada, K. Fukami, K. Murase, Cyanide-Free Displacement Silver Plating Using Highly Concentrated Aqueous Solutions of Metal Chloride Salts, J. Electrochem. Soc. 166 (2019) 409.

[42] J. K. Dennis, T. E. Such, Nickel and chromium plating, Elsevier Advanced Technology, Amsterdam, 2004.

[43] I. Nishida, K. Kimoto, Crystal habit and crystal structure of fine chromium particles: An electron microscope and electron diffraction study of fine metallic particles prepared by evaporation in argon at low pressures (III), Thin Solid Films. 23 (1974) 179.

[44] C. J. Doherty, J. M. Poate, R. J. H. Voorhoeve, Vacuum-evaporated films of chromium with the A-15 structure, J. Appl. Phys. 48 (1977) 2050.

[45] T. Tsuru, I. Takenaka, S. Kobayashi, T. Inui, Electrodeposition of Chromium from Chromium(III) Chloride Hexahydrate-Methanol Baths, J. Met. Finish. Soc. Japan. 28 (1977) 85. (doi: 10.4139/sfj1950.28.85)

Table I. Composition, pH, conductivity and viscosity of H_2O-LiCl-$CrCl_3$ electrolytes at 50 °C.

n = H_2O / LiCl (molar ratio)	composition (molar ratio) H_2O : LiCl : $CrCl_3$	pH	Conductivity / mS cm^{-1}	Viscosity / mPa s^{-1}
3	55.5 : 18.5 : 1.0	< 0	120.5	12.3
5	55.5 : 11.1 : 1.0	< 0	167.3	10.0
10	55.5 : 5.55 : 1.0	0.0	226	8.0
LiCl free	55.5 : 0 : 1.0	0.3	187	1.7

Table II. Composition, adjusted pH by adding concentrated HCl aq., conductivity and viscosity of H_2O-LiCl electrolytes at 50 °C.

n = H_2O / LiCl (molar ratio)	adjusted pH	Conductivity / mS cm^{-1}	Viscosity / mPa s^{-1}
3	0.0	147.5	7.1
5	0.1	238	2.7
10	1.0	285	1.3
100	1.0	63	0.7

Figure 1. Linear sweep voltammograms in H_2O-LiCl-$CrCl_3$ electrolytes at 50 °C for each H_2O / LiCl molar ratio n = 3, 5, 10 and LiCl-free system at a scan rate of 1 mV s^{-1}: (a) without ohmic compensation and (b) with ohmic compensation.

Figure 2. Linear sweep voltammograms for the blank tests in H_2O-LiCl-HCl electrolytes at 50 °C for each H_2O / LiCl molar ratio n of 3, 5, 10, 100 at a scan rate of 1 mV s^{-1}: (a) without ohmic compensation, and (b) with ohmic compensation.

Figure 3. Cyclic voltammograms in H_2O-LiCl-$CrCl_3$ electrolytes at 50 °C at a scan rate of 1 mV s^{-1} with switching potentials of –0.7 V, –1.0 V and –1.3 V for n = 3, 5, 10: a(i-iii) without ohmic compensation and b(i-iii) with ohmic compensation.

Figure 4. (a) Photographs and SEM images, (b) XRD patterns and (c) SEM-EDX spectra of the deposits prepared by galvanostatic electrolysis for n = 3 at 20 mA cm^{-2}, n = 5 at 40 mA cm^{-2}, and n = 10 at 40 mA cm^{-2}, without adding H_3BO_3.

Figure 5. (a) Photographs and SEM images, (b) XRD patterns and (c) SEM-EDX spectra of the deposits prepared by galvanostatic electrolysis for n = 3 at 20 mA cm^{-2}, n = 5 at 40 mA cm^{-2}, and n = 10 at 40 mA cm^{-2}, with addition of H_3BO_3.

Figure 6. HADDF-STEM images of the deposits prepared by galvanostatic electrolysis (a-i, a-ii) for n = 3, 5 without adding H_3BO_3 and (b-i, b-ii) with addition of H_3BO_3 for n = 3, 5; insets show the SAED patterns of crystalline white domains and amorphous black domains.

Figure 7. TEM-EDX spectra of the deposits prepared by galvanostatic electrolysis for n = 3 without H_3BO_3: (a) on the crystalline area and (b) on the amorphous area.

Figure 8. Photographs and the cross-sectional SEM images of the deposits prepared by galvanostatic electrolysis for 1h using H_2O-LiCl-$CrCl_3$ electrolytes with addition of H_3BO_3 for n = (a) 3 and (b) 5.

Figure 9. (a) Current efficiencies and (b) plating rates of chromium using H_2O-LiCl-$CrCl_3$ electrolytes with addition of H_3BO_3 for n = 3, 5.

Crystalline Chromium Electroplating with High Current Efficiency Using Chloride Hydrate Melt-Based Trivalent Chromium Baths

Ken ADACHI[a], Atsushi KITADA*[a], Kazuhiro FUKAMI[a]1, Kuniaki MURASE[a]1

[a] Department of Materials Science and Engineering

Kyoto University

Sakyo-ku, Kyoto 606-8501, Japan

* corresponding author; kitada.atsushi.3r@kyoto-u.ac.jp

1 ISE member

Table SI. Compositions of H_2O-$CaCl_2$-$CrCl_3$ and H_2O- $CaCl_2$ electrolytes and pH values at 50 ℃.

n = H_2O / $CaCl_2$ (molar ratio)	compositions (molar ratio) H_2O : $CaCl_2$: $CrCl_3$	pH
10	55.5 : 5.55 : 1.0	0.0 (as prepared)
10	55.5 : 5.55 : 0	0.0 (adjusted by adding HCl aq.)

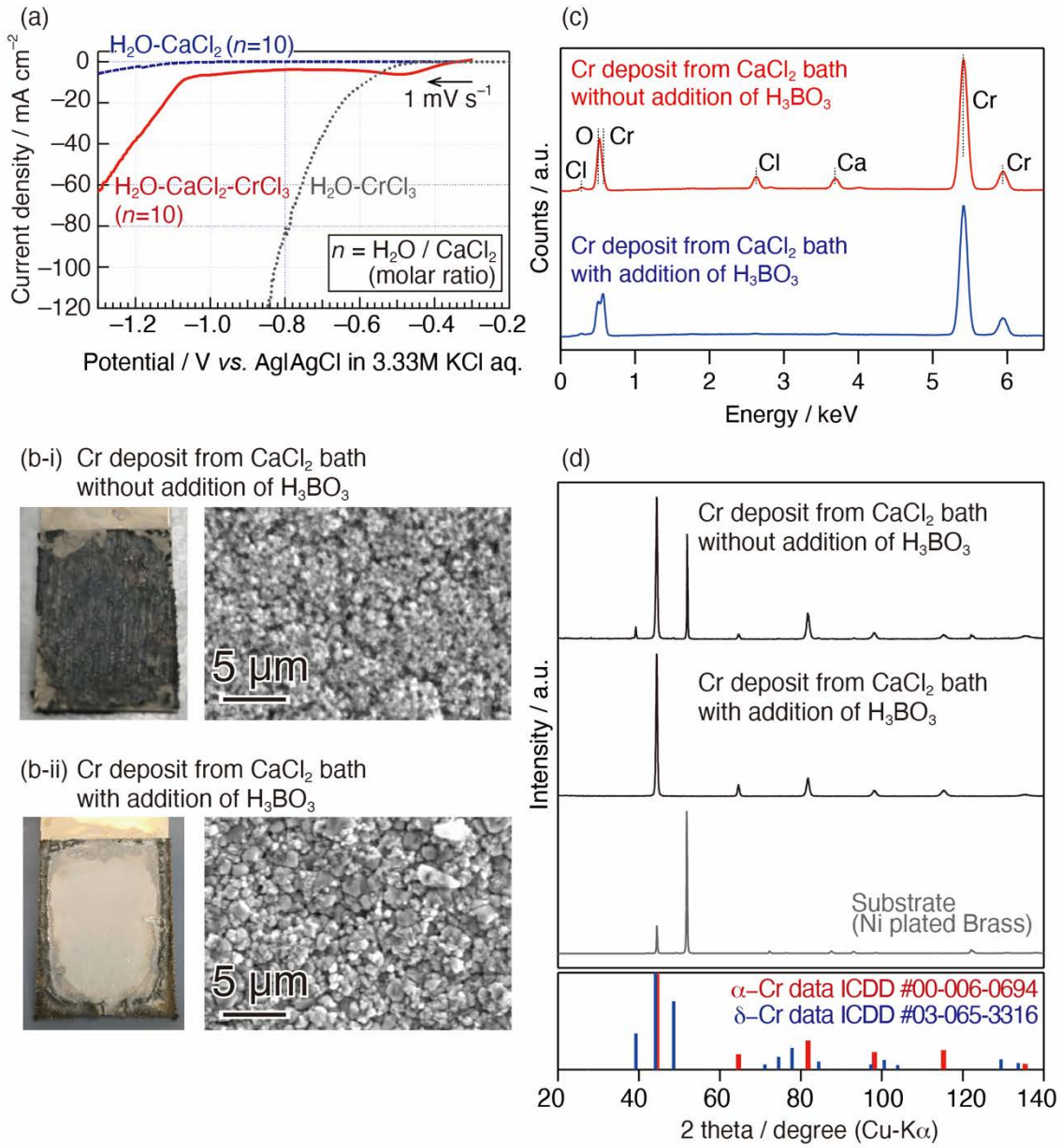

Figure S1. (a) Linear sweep voltammograms in H_2O-$CaCl_2$-$CrCl_3$ electrolyte and H_2O-$CaCl_2$ with $H_2O/CaCl_2$ molar ratio n = 10 at 50 °C at a scan rate of 1 mV s^{-1} without ohmic compensation, (b) photographs and SEM images, (c) EDX spectra, and (d) XRD patterns of the deposits prepared by galvanostatic electrolysis at 20 mA cm^{-2} for 1 h using H_2O-$CaCl_2$-$CrCl_3$ electrolyte n = 10 with and without addition of H_3BO_4.